

Grid Generation for Cascades Using Conformal Mapping

KENJI INOUE

National Aerospace Laboratory, Jindaiji, Chofu, Tokyo 182, Japan

Received November 5, 1982

A method of grid generation for cascades using conformal mapping is proposed. In this method, the transformation function which directly maps the domain of two periods of the cascade onto a rectangular region is determined numerically. The method is applied to the cases of high solidity without any difficulty. Once a fundamental O -type grid is obtained, either a through-flow grid or grids of C -type can be generated through it.

1. INTRODUCTION

The numerical calculation of a flow field needs a suitable treatment of the boundary condition which can be quite difficult to incorporate for complex geometries encountered in many problems. Good results are obtained when the boundaries correspond to grid surfaces. It is often desired for the coordinates to be orthogonal or nearly orthogonal and the mesh spacing to be directly controllable. In two dimensions, conformal mapping is a very powerful tool to generate such computational grids.

In the present paper, a method for grid generation for cascades using conformal mapping is proposed. Consider the highly regarded procedure developed by Ives and Liutermoza [1]. In their method, the first transformation maps the region exterior to the cascade of blades onto the region interior to a near circle and the second transformation maps the interior of the near circle onto the interior of a unit circle. When the solidity of the cascade is low, the first transformation produces a reasonable near circle but as the solidity increases, the contour tends to be peanut-shaped and the second transformation ceases to perform well. The method described in the present paper determines the transformation function mapping the region for two periods of the cascade of blades onto a rectangular region directly. The difficulty associated with the Ives-Liutermoza method, is thus eliminated.

The following assumptions are made: (1) the physical plane is $z = x + iy$ plane, the blades make a row in y direction, (2) the contour of one of the blades is given by a set of data $z_n = x_n + iy_n$ ($1 \leq n \leq N$, $z_N = z_1$), ordered in clockwise sense, (3) the coordinate x of the blade takes the values between -1 and 1 and the pitch of the blades in y direction is h .

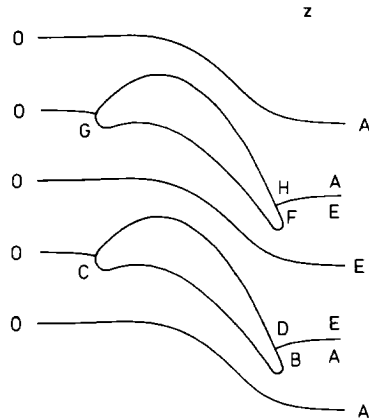


FIG. 1. Physical plane (z plane).

2. FUNDAMENTAL MAPPING (O -TYPE GRIDS)

We seek a transformation function mapping the region of the physical plane ($z = x + iy$ plane) for two periods of the cascade as shown in Fig. 1 onto an infinite strip on the computational plane ($\zeta = \xi + i\eta$ plane) (Fig. 2). The mapping function is assumed to have the form

$$z = A_0 \left[\frac{h}{\pi} \log \operatorname{sn}(\zeta, k) - 1 + \sum_{j=1}^J C_j \cosh(j-1) \frac{\pi \zeta}{K'} \right], \quad (1)$$

where A_0 is a real parameter which ultimately tends to one, $C_j = A_j + iB_j$ and k ($0 < k < 1$) are undetermined constants, K and K' the complete elliptic integrals of

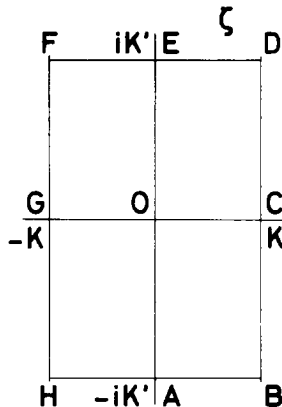


FIG. 2. Computational plane (ζ plane).

the first kind with the moduli k and $k' = (1 - k^2)^{1/2}$ respectively, sn one of the Jacobian elliptic functions. When

$$A_0 = 1, \quad k = \exp(-2\pi/h), \quad A_j = B_j = 0 \quad (j \geq 1), \quad (2)$$

expression (1) gives the mapping function for a cascade of flat plates of chord 2, pitch h , and zero stagger.

Putting $\zeta = K + i\eta$ in (1) and writing the real and imaginary parts separately, we obtain

$$\begin{aligned} x = A_0 & \left[-\frac{h}{\pi} \log \operatorname{dn}(\eta, k') - 1 + A_1 \right. \\ & \left. + \sum_{j=2}^J \left\{ A_j \cosh(j-1) \frac{\pi K}{K'} \cos(j-1) \frac{\pi\eta}{K'} \right. \right. \\ & \left. \left. - B_j \sinh(j-1) \frac{\pi K}{K'} \sin(j-1) \frac{\pi\eta}{K'} \right\} \right], \quad (3) \end{aligned}$$

$$\begin{aligned} y = A_0 & \left[B_1 + \sum_{j=2}^J \left\{ B_j \cosh(j-1) \frac{\pi K}{K'} \cos(j-1) \frac{\pi\eta}{K'} \right. \right. \\ & \left. \left. + A_j \sinh(j-1) \frac{\pi K}{K'} \sin(j-1) \frac{\pi\eta}{K'} \right\} \right], \quad (4) \end{aligned}$$

where dn is one of the Jacobian elliptic functions. The forms of (3) and (4) suggest an iterative method of solution. The origin of this iterative procedure may be found in the works of Imai [2, 3] for the cases of single airfoil.

The n th approximations $A_j^{(n)}$, $B_j^{(n)}$, and $k^{(n)}$ are assumed to be known.

(i) These values are substituted into (3) and the value of $A_1^{(n+1)}$ is so determined that $x_{\max} = -x_{\min}$. Then, the constant $A_0^{(n+1)}$ is so determined that $x_{\max} - x_{\min} = 2$. Using the data for the left-hand side of (3), we get the relation

$$\eta = \eta^{(n+1)}(x). \quad (5)$$

(ii) Using an appropriate constant ε_0 (typically 0.5), we replace $A_0^{(n+1)}$ by $(1 - \varepsilon_0)A_0^{(n)} + \varepsilon_0 A_0^{(n+1)}$.

(iii) Using $A_0^{(n+1)}$, we get $k^{(n+1)}$ by

$$\log k^{(n+1)} = A_0^{(n+1)} \log k^{(n)}. \quad (6)$$

A_0 tends to one as the approximation goes on.

(iv) Though the profile of the blade is given in the form $y(x)$, relation (5) enables us to write y as a function of η ,

$$y = y^{(n+1)}(\eta).$$

This is used for the left-hand side of (4) and the Fourier analysis gives

$$A_j^{(n+1)} = \frac{1}{K'A_0 \sinh[(j-1)\pi K/K']} \int_{-K'}^{K'} y \sin[(j-1)\pi\eta/K'] d\eta \quad (j \geq 2),$$

$$B_j^{(n+1)} = \frac{1}{K'A_0 \cosh[(j-1)\pi K/K']} \int_{-K'}^{K'} y \cos[(j-1)\pi\eta/K'] d\eta \quad (j \geq 1).$$

(v) With an appropriate constant ε_1 (typically 0.1), $A_j^{(n+1)}$ and $B_j^{(n+1)}$ are replaced by $(1 - \varepsilon_1)A_j^{(n)} + \varepsilon_1 A_j^{(n+1)}$ and $(1 - \varepsilon_1)B_j^{(n)} + \varepsilon_1 B_j^{(n+1)}$.

The procedure (i)–(v) is repeated until the required convergence is attained. The values for the cascade of flat plates (2) are taken as the first approximation. Steps (iii) and (v) of the procedure prevent the divergence of the successive approximation and ε_0 and ε_1 are relaxation constants.

Examples of grids generated by the present method are shown in Figs. 3 and 4. In these grids, the lines of constant ξ encircle the blades and the grids are called *O*-type. Across the periodic boundaries *OA* and *OE*, the lines of constant η continue smoothly. As the solidity increases, the constant k decreases and K'/K increases. The present method does not break down for the solidity as high as 2.9.

Here, the derivation of (6) is described. In order that the pitch of the cascade in z plane equals h , A_0 must be one. Also $k^{(n+1)}$ is determined so that

$$A_0 \log \operatorname{dn}(\eta, k^{(n)}) = \log \operatorname{dn}(\eta, k^{(n+1)}). \quad (7)$$

Relation (2) for the case of flat plates suggests that when the solidity is not small,

$$k' \doteq 1 \quad \text{and} \quad \operatorname{sn}(\eta, k') \doteq \tanh \eta.$$

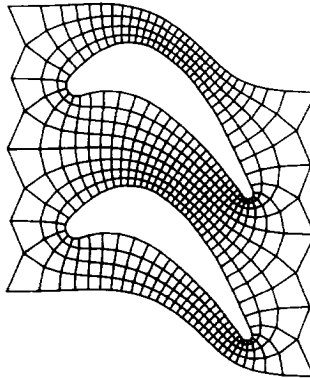


FIG. 3. Example of *O*-type grid (1). Solidity 1.58, $N = 42$, $J = 20$, $\varepsilon_0 = 0.5$, $\varepsilon_1 = 0.1$, $k = 4.10 \times 10^{-5}$, $K = 1.57$, $K' = 11.5$.

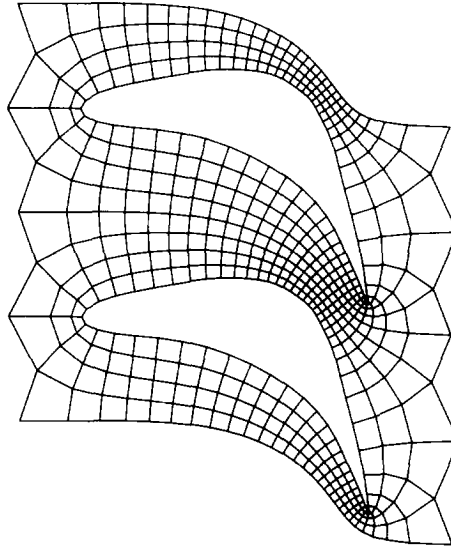


FIG. 4. Example of O -type grid (2). Solidity 1.73, $N = 32$, $J = 10$, $\varepsilon_0 = 0.5$, $\varepsilon_1 = 0.1$, $k = 1.59 \times 10^{-5}$, $K = 1.57$, $K' = 12.4$.

Then, for a wide range of η ,

$$\operatorname{sn}(\eta, k') \doteq 1$$

and

$$\operatorname{dn}(\eta, k') = [1 - k'^2 \operatorname{sn}^2(\eta, k')]^{1/2} \doteq k.$$

Putting this into (7), we obtain

$$\log k^{(n+1)} = A_0 \log k^{(n)}.$$

3. THROUGH-FLOW GRIDS

The mapping function obtained in the preceding section can be used to generate grids of other types. First, we treat a grid in which one family of the grid curves represents the streamlines of a flow through the cascade from left to right as shown in Fig. 5 (through-flow grids). We consider the complex velocity potential $Z = X + iY$ of a flow induced by a distribution of sources and sinks on the ζ plane,

$$\begin{aligned} \text{unit sinks at } \zeta &= 2mK + i2nK', \\ \text{unit sources at } \zeta &= 2mK + i(2n - 1)K', \end{aligned} \quad (8)$$

with $m, n = 0, \pm 1, \pm 2, \dots$,

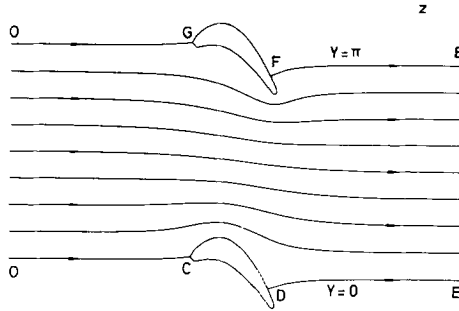


FIG. 5. Streamlines of the flow which generates a through-flow grid.

as shown in Fig. 6. The through-flow grid is based on the X and Y coordinates. The flow induced by the distribution (8) is expressed as

$$Z = \log \operatorname{sn}(\zeta, k).$$

Solving for ζ , produces

$$\zeta = \int_0^{\exp Z} [(1-t^2)(1-k^2t^2)]^{-1/2} dt.$$

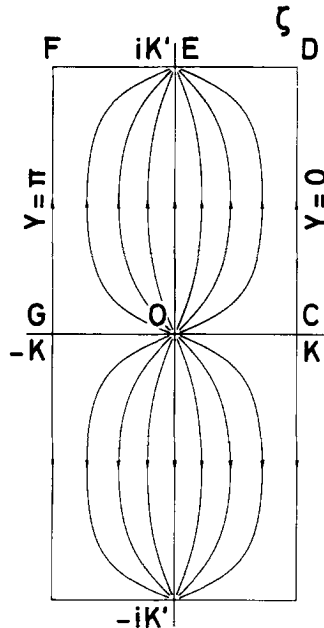


FIG. 6. Distribution of sources and sinks on ζ plane which generates a through-flow grid.

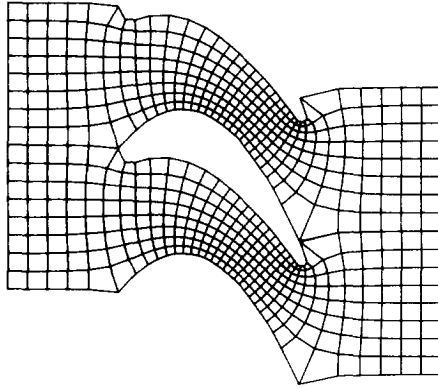


FIG. 7. Through-flow grid for the cascade; same as shown in Fig. 3.

At the stagnation points of the flow $\zeta = K$ and $K + iK'$,

$$Z(K) = 0 \quad \text{and} \quad Z(K + iK') = -\log k.$$

In Fig. 7, an example of the through-flow grid for the same cascade shown in Fig. 3 is shown. The grid continues smoothly across the periodic boundaries OC , OG , DE , and FE .

4. C-TYPE GRIDS I

Next, consider a grid in which a family of coordinate lines represents the streamlines of a flow starting from infinity to the right, encircle the blades, and returning to infinity to the right (Fig. 8). The flow, due to a distribution of sources and sinks on ζ plane, has

$$\text{unit sources at } \zeta = 2mK + i(4n - 1)K',$$

$$\text{unit sinks at } \zeta = 2mK + i(4n + 1)K',$$

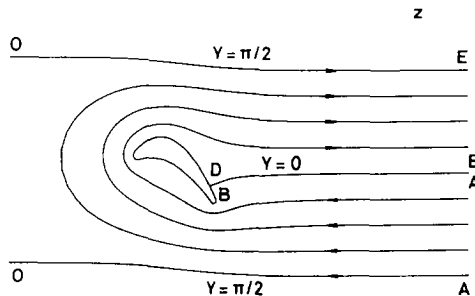


FIG. 8. Streamlines of the flow which generates a C-type grid.

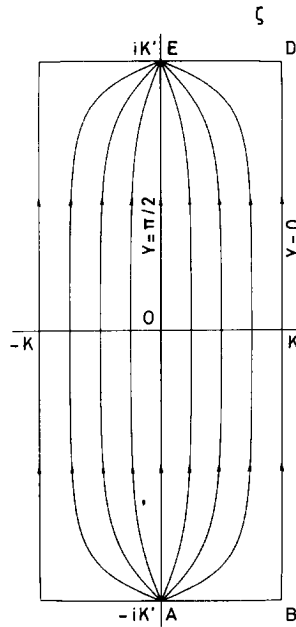


FIG. 9. Distribution of sources and sinks on ζ plane which generates a C-type grid.

as shown in Fig. 9. The complex velocity potential Z of the flow is given by

$$Z = X + iY = \log \operatorname{sn} \left[\frac{K_1}{K} (\zeta + iK'), k_1 \right]. \tag{9}$$

The constants K_1 and k_1 satisfy the relation

$$K_1/K_1 = 2K'/K,$$

where K_1 and K'_1 are the complete elliptic integrals of the first kind with the moduli k_1 and $k'_1 = (1 - k_1^2)^{1/2}$, respectively. The modulus k_1 is determined as

$$k_1 = (1 - k')/(1 + k'),$$

where Landen's transformation formula is used. Solving expression (9) for ζ , gives

$$\zeta = \frac{K}{K_1} \int_0^{\exp Z} [(1 - t^2)(1 - k_1^2 t^2)]^{-1/2} dt - iK'.$$

At the stagnation points $\zeta = K \pm iK'$,

$$Z(K - iK') = 0 \quad \text{and} \quad Z(K + iK') = -\log k_1$$

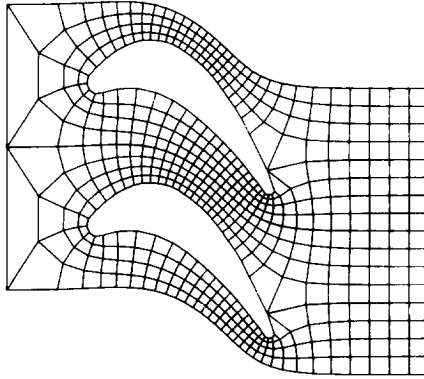


FIG. 10. C-type grid for the cascade: same as shown in Fig. 3.

hold. An example of C-type grid generated by this method is shown in Fig. 10. The cascade is the same as that shown in Fig. 3. The grid lines of constant X continue smoothly across the periodic boundaries OA , OE and the cut BA (DE).

5. C-TYPE GRIDS II

A generalized grid with cut BA , departs from a given point z_s on the blade (e.g., the trailing edge; Fig. 11), is useful for calculating flows in the boundary layer and the wake with a great accuracy. Consider a flow induced by a distribution of vortices on ζ plane, given by vortices of intensity κ at

$$\zeta = 4mK + i(4n - 1)K', (4m - 2)K + i(4n + 1)K',$$

vortices of intensity $-\kappa$ at

$$\zeta = (4m - 2)K + i(4n - 1)K', 4mK + i(4n + 1)K',$$

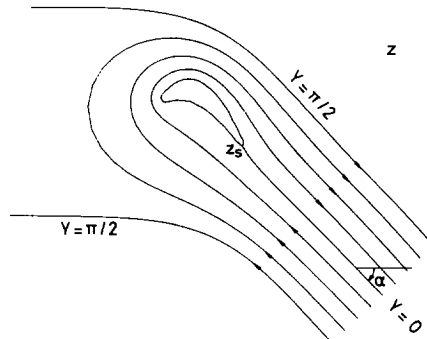


FIG. 11. Streamlines of the flow which generates a grid of C-type II.

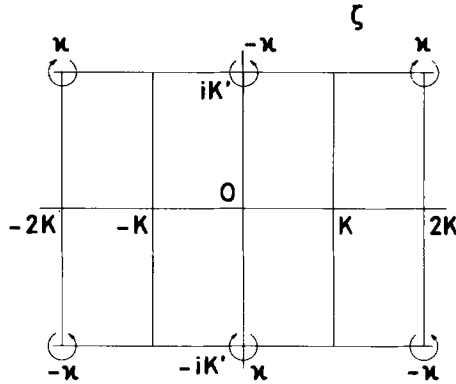


FIG. 12. Distribution of vortices on ζ plane which is used for the generation of a grid of C-type II. Case $\kappa < 0$.

where the sign of κ is defined as positive when the rotation of the flow due to the vortex is counterclockwise (Fig. 12). The desired grid is obtained by the superposition of this flow and that described by (9) (Fig. 13). The complex velocity potential of the resulting flow is expressed as

$$Z = \log \operatorname{sn} \left[\frac{K_1}{K} (\zeta + iK'), k_1 \right] - i\kappa \log \frac{\operatorname{cn} \left[\frac{1}{2}(\zeta - iK'), k \right] \operatorname{sn} \left[\frac{1}{2}(\zeta + iK'), k \right]}{\operatorname{sn} \left[\frac{1}{2}(\zeta - iK'), k \right] \operatorname{cn} \left[\frac{1}{2}(\zeta + iK'), k \right]}, \quad (10)$$

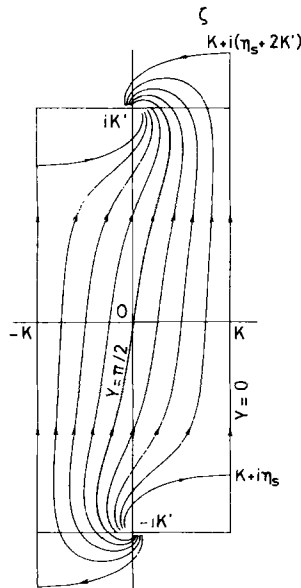


FIG. 13. Streamlines of the flow which generates a grid of C-type II. Case $\kappa < 0$.

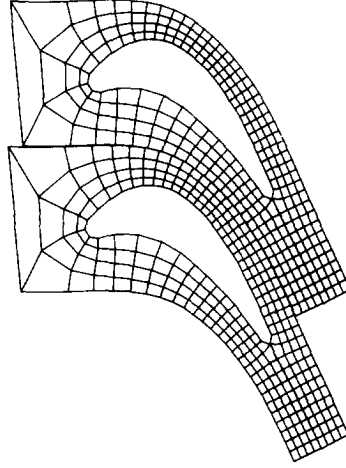


FIG. 14. Grid of *C*-type II for the cascade same as shown in Fig. 3. $\varepsilon_3 = 0.1$, $\eta_3 = -10.0$, $\kappa = -2.05$, $\alpha = -64.0^\circ$.

where cn is one of the Jacobian elliptic functions. The constant κ is determined so that $\zeta_s = \zeta(z_s) = K + i\eta_s$ is a stagnation point, i.e.,

$$(dZ/d\zeta)_{\zeta=\zeta_s} = 0.$$

The value of ζ_s is obtained by solving $z(\zeta_s) = z_s$ numerically. Using the properties of the functions $Z(\zeta)$ and $z(\zeta)$, when

$$\zeta \rightarrow \pm iK', \quad \frac{dZ}{dz} \rightarrow \pm \frac{\pi}{h} (1 - i\kappa),$$

we note that the line $Y = 0$ makes an angle α ,

$$\alpha = \tan^{-1} \kappa$$

with x axis as $x \rightarrow \infty$. Because expression (10) cannot be solved explicitly with respect to ζ , iterative methods are employed to obtain the values of ζ corresponding to a given Z . When employing successive approximation, the value at a neighbouring point is assumed as the first approximation. But near $\zeta = \pm iK'$, Z varies rapidly, therefore some relaxation procedure (with a relaxation constant ε_2 , typically 0.1) like (iii) and (v) in the case of *O*-type is applied in order to converge to the solution.

An example of *C*-type grid generated by this method is shown in Fig. 14. The cascade is the same as that shown in Fig. 3. The lines of constant X continue smoothly across the cut BA (DE) but are discontinuous across the periodic boundaries OA and OE .

ACKNOWLEDGMENTS

The author thanks Dr. A. Tamura (NAL) who suggested the subject, Mr. T. Suzuki (Systems Design) who conducted the programming, and Mr. M. Fukuda (NAL) who assisted in numerical computation.

REFERENCES

1. D. C. IVES AND J. F. LIUTERMOZA, *AIAA J.* **15** (1977), 647.
2. I. IMAI AND K. SATO, *J. Aero. Res. Inst., Tokyo Imp. Univ.* **247** (1945), 91. [Japanese]
3. I. IMAI, I. KAJI, AND K. UMEDA, *J. Fac. Sci., Hokkaido Univ. Ser. II* **3** (1950), 265.